Amiloride-Insensitive Cation Conductance in *Xenopus laevis* Olfactory Neurons: A Combined Patch Clamp and Calcium Imaging Analysis

Detlev Schild and Fritz Walter Lischka

Physiologisches Institut, Universität Göttingen, D-37073 Göttingen, Germany

ABSTRACT   We used digital calcium imaging with Fura-2 in conjunction with the tight-seal whole-cell patch clamp technique to describe a novel cation conductance in olfactory neurons of the clawed toad *Xenopus laevis*. Substitution of extracellular Ca^{2+} and Na^+ was used as a tool to change $[Ca^{2+}]_i$. When $[Ca^{2+}]_i$ was increased to about 450 nM, a conductance g_{cat} activated that was permeable for cations. Upon g_{cat} activation, an increase in $[Ca^{2+}]_i$ occurred in the dendritic knob. Once activated, g_{cat} showed no further dependence upon $[Ca^{2+}]_i$. I_{cat} is shown to be different from the current activated by a mixture of the odorants citralva and amyl acetate. We conclude that there are two different cation conductances in the peripheral compartments of olfactory neurons in *X. laevis*.

INTRODUCTION

Not many years ago olfactory transduction was thought to be one signal cascade including receptor proteins, G-proteins, adenylate cyclase, formation of cAMP, and direct gating of a cyclic nucleotide-activated cation conductance g_{cn} (Firestein et al., 1991). Recent evidence suggests a growing complexity of olfactory transduction: 1) in many species, there is now convincing evidence for the existence of an IP_3-mediated olfactory transduction pathway (Fadool and Ache, 1992; Restrepo et al., 1990; Restrepo et al., 1992); 2) a calcium-dependent chloride conductance (Kleene and Gesteland, 1991) appears to contribute to odorant-induced conductance changes (Kurahashi and Yau, 1993); 3) cGMP might play a physiological role (Breer et al., 1992; Lischka and Schild, 1993a); 4) the sensitivity of g_{cn} to cAMP appears to be modulated by $[Ca^{2+}]_i$ (Lynch and Lindemann, 1992); and 5) there might be interactions between the IP_3-mediated and the cAMP-mediated pathways (Ronnett and Snyder; 1992, Frings, 1993). In amphibians, where the cAMP-mediated pathway had been established first (Firestein and Werblin, 1989), there are now some indications for the involvement of IP_3 in olfactory transduction (Schild et al., 1992; Bacigalupo et al., 1993).

In the clawed toad some odorants such as citralva and amyl acetate activate the cAMP-gated cation conductance g_{cn} which can also be activated by cGMP and sodium nitroprusside (Lischka and Schild, 1993a). We now report evidence for a ciliary cation conductance g_{cat} in *Xenopus laevis* olfactory neurons, which can be activated by $[Ca^{2+}]_i$, which is permeable for Ca^{2+} and which is different from the cyclic nucleotide activated conductance g_{cn}.

MATERIALS AND METHODS

Preparation and tissue dissociation

The procedures were very similar to those described previously (Schild, 1989). Briefly, adult *X. laevis* were decapitated after anesthesia in a mixture of water and ice. The olfactory organs were removed and put into the dissociation solution (see below). Enzymes were not applied to prevent alterations of membrane proteins involved in the transduction process. The mucosae were then mechanically disrupted in a drop of dissociation solution (~50 μl), triturated with a plastic pipette (2 mm i.d.), and then 100 μl of Ringer's solution was added to the cell suspension. The cells were stored at 5°C and used within 6 h. Fifty μl of the cell suspension were put onto a glass coverslip within the experimental chamber (volume 100 μl). Coverslips were coated with Concanavalin A (0.3 mg/ml). Only cells which had retained their cilia during the dissociation procedure were used.

Patch clamp whole-cell configuration

All patch clamp experiments were done in the whole-cell configuration (Hamill et al., 1981) and the procedures were identical to those reported previously (Schild and Bischofberger, 1991). Electrodes of 7 MΩ resistance were fabricated from borosilicate glass (1.8 o.d., Hilgenberg, Malsfeld, Germany) using a custom-made two-stage electrode puller.

The patch clamp setup consisted of an EPC7 amplifier (List, Darmstadt, Germany), a PCM unit (Instrutech VR100) with video recorder, and a VME computer (Eurocom5, ELTEK, Darmstadt, Germany). The voltage clamp pulse protocol program was written in C language and ran on a secondary processor board (SAC7, ELTEK) in the VME computer, which delivered the command signals to a 12-bit digital-to-analog converter. The resulting pulses were fed to the patch clamp amplifier. Seal resistances were in the range of 0.5 and 20 GΩ. Whole-cell breakthrough was achieved by brief suction pulses or by short negative voltage pulses. All recordings were done within 6 h after preparation.

Solutions

The bath solutions used are listed in Table 1. The free Ca^{2+} was measured in all bath solutions using a calcium-sensitive electrode (Ingold, Steinbach, Germany), giving values between 0.8 and 60 μM.

The following pipette solutions were used (concentrations in mM). So-lution 1 (I1): potassium aspartate, 72; sodium gluconate, 20; $MgCl_2$, 3; K_2-ATP, 1; K_5-Fura-2, 0.2; Hepes, 10. Solution 2 (I2): KCl, 79; NaCl, 5; $MgCl_2$, 5; K_2-ATP, 1; cGMP, 0.2*10–3; EGTA, 2; K_5-Fura-2, 0.2; Hepes, 1.

All solutions at pH 7.8; osmolarity in bath and pipette solutions was 230 and 180, respectively. In our hands, the osmolarity ranges within which *X*.

TABLE 1 Bath solutions

Solution	NaCl	KCl	MgCl₂	Choline chloride	Choline tartrate	TEA chloride	Sucrose	Hepes
Dissociation solution	116	2.5						1
Frog Ringer's R1, 115/0	115	4	0.5					1
RCh, 0/0		4	0.5	117				1
RT		4	0.5	19	69			1
RTEA		4	0.5			115		1
RS			0.5				225	1

All concentrations are millimolar.

laevis olfactory cells retain their normal morphology under whole-cell conditions are 215–230 mOsmol and 180–190 mOsmol, respectively. The health of the cells was ascertained by exclusion of trypan blue, low calcium concentration (<100 nM) at the beginning of recording, and by occasionally checking the voltage-gated whole-cell currents during the experiments.

In some plots solutions are abbreviated by their sodium and calcium concentrations (115/0 for R1, etc.). Where indicated in the text, 1 mM $CaCl_2$, 1 mM amiloride, or 5 mM $NiCl_2$ were (isosmotically) added to a solution.

A mixture of citralva (100 μM) and amyl acetate (100 μM) were dissolved in R1 and applied through a second pipette onto the cilia.

CCD camera imaging and measurement of intracellular calcium

A 150-watt xenon arc lamp (Amko, Tornesch, Germany)) was used for exciting the Ca indicator dye Fura-2 at 340 and 380 nm. The light passed through an infrared filter (quartz windows, water, 7 cm path length) and was coupled through a ultraviolet light guide to a filter wheel (Luigs & Neumann, Ratingen, Germany), which was mounted on an inverted microscope (Zeiss Axiovert 35). The filter wheel held interference filters for 340 and 380 nm (Lys&Optik, Lyngby, Denmark) and was driven by a step motor. Its three positions (340 nm, 380 nm, or dark) were set by an electronic controller and computer programs integrated into the imaging software. The software modifications as well as the filter wheel controller were custom made.

The fluorescent light emitted from the cells was first separated from the excitation light by a dichroic beam splitter at 395 nm mounted below the objective (Zeiss 63*/1.25, oil) and then passed through a barrier filter at 500–530 nm. The fluorescence images were captured by a slow-scan CCD camera (16 bits/pixel; Photometrics, CE 200, Tucson, Arizona) and read into the VME computer. The CCD readout frequency was 40 kHz. Rather than taking full frame images, we usually read subarrays of the CCD array of about 100 × 150 pixels, which contained the entire cell. Integration time varied between 500 and 3000 ms according to dye loading conditions. The background value of an image was calculated after subtraction of a dark image (closed shutter of the camera) from the intensity histogram of the corresponding image.

$[Ca^{2+}]_i$ was estimated from the ratio of background-corrected images according to the algorithm described by Grynkiewicz et al. (1985). Calibration was performed in situ, i.e., pipette solutions with a very low $[Ca^{2+}]_i$ (10 mM EGTA, nominally no Ca^{2+}), a known $[Ca^{2+}]$ (105 nM, as determined by a Ca^{2+}/Bapta mixture; Marks and Maxfield, 1991), and a high $[Ca^{2+}]_i$ concentration (10 mM) were used to measure and calculate the corresponding fluorescence intensities and ratios, respectively. in the case of known $[Ca^{2+}]_i$, it was assumed that the cellular calcium control mechanisms did not markedly affect the calibration because a high Bapta concentration (10 mM) was used.

Calibration resulted in constants $R_{min} = 0.05$, $R_{max} = 1.6$, and apparent $K_d^* = 1117$ nM. Using the pipette calibration solutions with low and high $[Ca^{2+}]_i$ at 380 nm, the ratio of the resulting fluorescence values was 8.4. Considering the ionic strength of 0.1 M of our pipette solutions, the resulting K_d of Fura-2 with respect to calcium, i.e., $K_d = 1117/8.4 = 133$ nM, was comparable with the value reported by Grynkiewicz et al. (1985). Calcium concentrations were then calculated according to (Grynkiewicz et al., 1985)

$$[Ca^{2+}]_i = K_d^*(R - R_{min})/(R_{max} - R).$$

The calibration measurements were repeated several times and the results were pooled. They are valid only under our particular experimental configuration of filters, objective, illumination, etc. We also performed calibration measurements in droplets of the above given solutions. The resulting calibration constants led, however, to values for $[Ca^{2+}]_i$ that were considerably lower than in the in situ calibration. We used the in situ calibration because calibration and recording conditions were similar to each other.

The images were directly viewed during the experiments and then sent to a SUN SPARC workstation I for subsequent processing and viewing.

RESULTS

When the intracellular concentration of calcium in *X. laevis* olfactory cells was increased from resting levels to a value of about 400 nM, 39 of 74 tested cells developed an inward current I_{cat} at a voltage clamp holding potential of −80 mV (Fig. 1). Associated with this inward current was a concomitant, non-transient increase of $[Ca^{2+}]_i$ in the dendritic knob (Fig. 2). This suggested that the inward current occurred in the peripheral compartments of the cell and that the under-
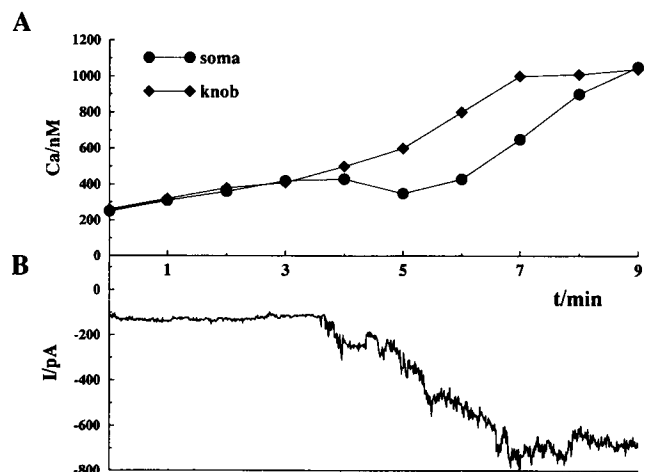

FIGURE 1 Simultaneous record of $[Ca^{2+}]_i$ and voltage clamp current in an olfactory neuron of *X. laevis*. The seal resistance before breaking through into the whole-cell mode was 0.6 GΩ. Under this condition, a slow increase in $[Ca^{2+}]_i$ occurred as described in the text. (A) $[Ca^{2+}]_i$ was measured in the soma and the dendritic knob. After a steady increase in $[Ca^{2+}]_i$ over 3 min, during which $[Ca^{2+}]_i$ in the knob and the soma were identical, $[Ca^{2+}]_i$ in the dendritic knob increased more rapidly. This increase in $[Ca^{2+}]_i$ in the knob was followed by an increase in the soma, and at $t = 9$ min, $[Ca^{2+}]_i$ is again identical in soma and knob. (B) At a time when $[Ca^{2+}]_i$ in the knob was about 420 nM, the inward current at the holding potential of −73 mV increased and reached a steady-state amplitude of about 700 pA after about 200 s. Bath solution R1; pipette solution I1.

FIGURE 2   Spatial distribution of $[Ca^{2+}]_i$ during the experiment shown in Fig. 1. The images (from *left* to *right*) were taken at $t = 3, 5, 7$, and 9 min of the time axis of Fig. 1. $[Ca^{2+}]_i$ is color-coded from 0 nM (*dark blue*) to 1200 nM (*red*). While the spatial distribution of $[Ca^{2+}]_i$ is generally homogeneous in the first (*left*) image, in the second image ($t = 5$ min) a conspicuous increase in $[Ca^{2+}]_i$ is seen in the dendritic knob and $[Ca^{2+}]_i$ is slightly increased in the distal dendrite. Two minutes later, $[Ca^{2+}]_i$ in the whole dendrite and to a lesser extent in the soma is markedly increased. At $t = 9$ min, $[Ca^{2+}]_i$ is uniformly high (about 1.1 μM) in soma and dendrite.

lying conductance was permeable for calcium ions. In standard Ringer's solution (R1), the activation of I_{cat} was always accompanied by an increase of $[Ca^{2+}]_i$ in the dendritic knob (seen in 18 of 18 tested cells). The range of $[Ca^{2+}]_i$ in which I_{cat} occurred varied from cell to cell. To describe this range, we measured the calcium concentration in the dendritic knob Ca_k^{2+} (= $[Ca^{2+}]_i$ measured in the knob) in the two images that immediately preceded and followed the activation of I_{cat}. The resulting distributions are plotted as histograms in Fig. 3 and showed that Ca_k^{2+} before activation of I_{cat} never ex-

FIGURE 3   Distributions of $[Ca^{2+}]_i$ in the dendritic knob before (A) and after (B) activation of I_{cat}. Data were taken from 18 cells. The histograms give the relative frequency p of cells that had a calcium concentration in the range indicated on the abscissa (binwidth 100 nM). Data in the upper histograms (A) were taken from the last images before activation of I_{cat} (e.g., the first image in Fig. 2), and data in the lower histogram (B) were taken from the first images after activation of I_{cat} (e.g., the second image in Fig. 2). $[Ca^{2+}]$ before activation of I_{cat} was always lower than 500 nM, whereas it was always higher than 400 nM after activation.

ceeded 500 nM and that Ca_k^{2+} after activation of I_{cat} was in all cases higher than 400 nM. I_{cat} was thus activated between 400 and 500 nM.

This range of $[Ca^{2+}]_i$ is about one order of magnitude higher than the resting concentrations reported by Restrepo et al. (1990) and by Lischka and Schild (1993b). However, resting $[Ca^{2+}]_i$ is easily underestimated, first, because the K_d of Fura-2 may be different in cytoplasm than in saline solution (Restrepo and Teeter, 1990) and second, because the concentrations of Fura-2 necessary to obtain sufficiently large fluorescence signals buffer $[Ca^{2+}]_i$ at low levels. The added buffer Fura-2 might even dominate over the endogenous Ca^{2+} buffer. This effect has been analyzed in detail in chromaffin cells (Neher and Augustine, 1992). A further indication that $[Ca^{2+}]_i$ reaches levels considerably higher than the reported resting concentrations is that the Ca^{2+}-activated chloride conductance in these cells appears to be half activated at 5 μM (Kleene and Gesteland, 1991).

Once I_{cat} was activated in solution R1 (18 of 32 cells), $[Ca^{2+}]_i$ gradually increased not only in the dendritic knob, but the increase spread into the other compartments of the neuron (Fig. 2). After some minutes, the shape of the cells changed, beginning with a swelling and retraction of the peripheral dendrite (Fig. 2, *right*). With choline$^+$ in the bath (42 cells), I_{cat} developed in 21 cells; the current amplitudes were, however, considerably smaller than in solution R1. The peripheral increase in $[Ca^{2+}]_i$ was also much smaller and detectable only in 8 of 21 cells. Morphological changes as described occurred only rarely under these conditions. We therefore conducted most of the following experiments with choline$^+$ as the main cation in the bath solution.

The activation of I_{cat} did not depend on the particular condition under which $[Ca^{2+}]_i$ was increased to a value of about 450 nM. Three different conditions were observed: $[Ca^{2+}]_i$ increased 1) if the seal resistance was in the range of or lower than 0.7 GΩ (9 cells); 2) if ATP was omitted from the pipette solution (23 cells) (Lischka and Schild, 1993b); and 3) if we decreased Na$^+$ and increased $[Ca^{2+}]_i$ in the bath (42 cells). In the first case, activation of g_{cat} was observed in 6 cells (see Figs. 1 and 2 for an example). The latter method was our standard experimental procedure. Under this condition I_{cat} activated in 21 of 42 cells. Fig. 4 shows a representative example: in solution 0/1 $[Ca^{2+}]_i$ increased to about 450 nM and then activated I_{cat}. When $[Ca^{2+}]$ in the bath was removed (solution 0/0 with nominally no Ca^{2+}, actually 25 μM, as measured with an ion-selective electrode), $[Ca^{2+}]_i$ decreased to about 100 nM, but I_{cat} once activated by $[Ca^{2+}]_i$ did not appear to depend further upon $[Ca^{2+}]_i$ and stayed about constant. In three other cells, we added 1 mM EGTA to solution 0/0 and applied this solution for 1 min without any effect upon I_{cat} (data not shown). As a calcium-dependent chloride conductance has been described in amphibian olfactory cells (Kleene and Gesteland, 1991, Kurahashi and Yau, 1993), we checked whether or not a chloride current was superimposed on I_{cat}. In the experiment shown in Fig. 4, we replaced choline chloride by choline tartrate, thereby shifting E_{Cl} from
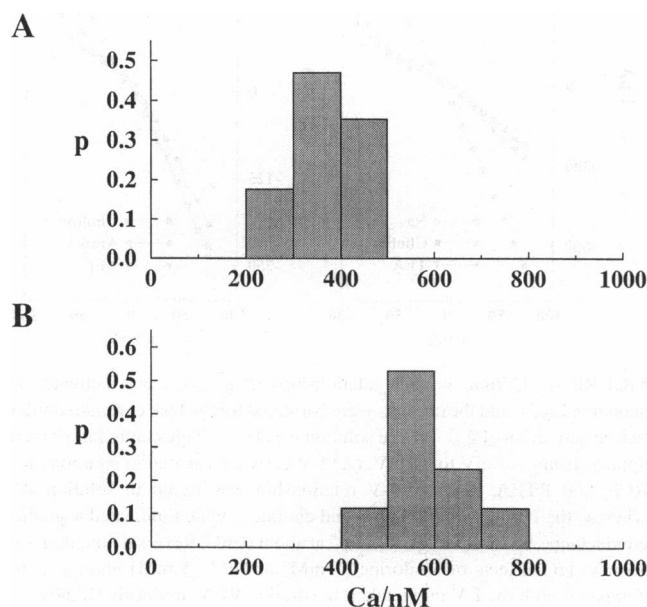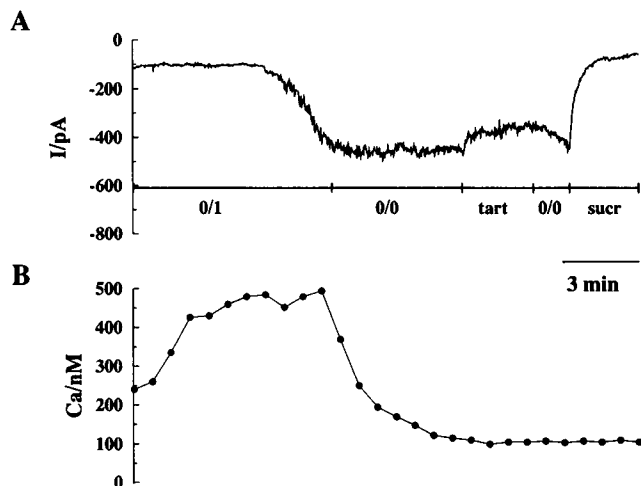
A

B

FIGURE 4 Simultaneous record of current (A) and [Ca^{2+}] in the dendritic knob (B) of an olfactory neuron. At the beginning of the experiment (t = 0), Ringer's solution R1 was replaced by solution 0/1 (same as solution 0/0, plus 1 mM $CaCl_2$). In response to this substitution, [Ca^{2+}]$_i$ increased to about 480 nM (B), and an inward current I_{cat} activated (A). Voltage clamp holding potential was u_h = −73 mV. In solution 0/0 (choline$^+$ and 25 μM Ca^+ in the bath) the inward current I_{cat} persisted, though [Ca^{2+}]$_i$ decreased to a steady-state concentration of about 100 nM. Replacing chloride$^-$ by tartrate$^-$ reduced the inward current reversibly and I_{cat} was abolished in solution RS. Pipette solution I1.

−73 mV to −33 mV. Under these conditions, a chloride conductance would have resulted in a larger inward current. Instead, the inward current was reduced by about 22%, which can be explained by a shift in the junction potential at the indifferent electrode (15 mV as measured in control experiments). We therefore concluded that there was no significant chloride current under the given circumstances. At the end of the experiment we replaced solution 0/0 by a solution in which choline chloride was isosmotically replaced by sucrose. Sucrose in the bath abolished I_{cat} completely.

In nine olfactory neurons, sucrose was locally applied through a second pipette onto single compartments of the cells. The effect of sucrose upon I_{cat} strongly depended upon the position of the application pipette (Fig. 5, *inset*). The current trace shows a cell in which I_{cat} was markedly reduced with the sucrose solution applied onto the cilia, consistent with g_{cat} localization predominantly on the peripheral compartments of the cell, while no current reduction was measured with the application pipette directed onto the soma. In cells with short dendrites (<40 μm), a reduction of I_{cat} also occurred with sucrose applied onto the soma, but it was consistently smaller than with sucrose applied to the dendritic knob (data not shown). This was not unexpected, because the sucrose plume also affected the bath composition around the dendritic knob and the cilia.

The conductance underlying I_{cat} was permeable to a number of cations, including large cations such as choline$^+$ and TEA$^+$. Current voltage relationships of I_{cat} were measured using a ramp clamp protocol and showed a reversal potential of about 15 mV (Fig. 6 A).
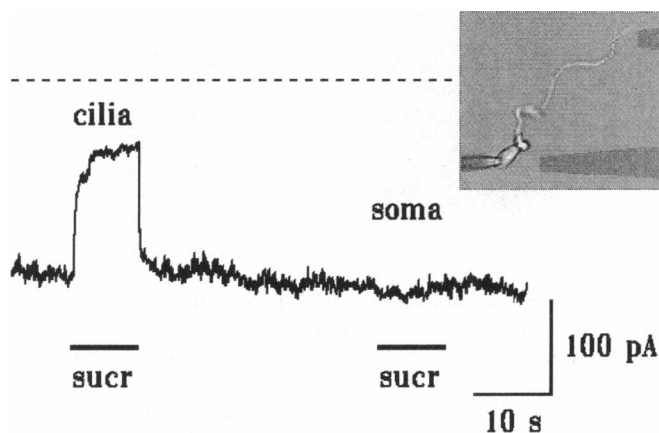

FIGURE 5 Effect of local application of sucrose on the soma and the cilia of an olfactory neuron. (*Inset*) an image of the cell from which the record was taken is shown with the two pipette positions used. Silhouettes added later on the picture. With the inward current I_{cat} activated (u_h = −73 mV) as shown in the preceding figure, solution RS was applied from a second pipette onto the cilia at the time indicated by the first bar below the current trace. While in this case a large reduction in I_{cat} is obvious, no reduction at all occurred when solution RS was applied to the soma. In this cell, the reduction of I_{cat} as well as the lack of current reduction was observed three times. The dashed line indicates the steady-state current level before I_{cat} activated. Pipette solution I2; bath solution R1.
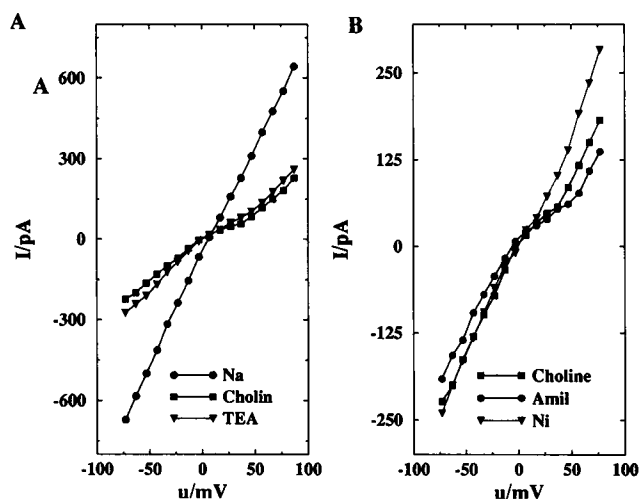
A

B

FIGURE 6 Current voltage relationships of g_{cat}. I_{cat} was activated as shown in Fig. 4, and the currents were corrected for the leak current recorded before activation of g_{cat}. Pipette solution was I1. Voltage clamp ramps were applied from −73 mV to 87 mV. (A) I-V curves measured in solutions R1, RCh, and RTEA. A linear I-V relationship was found in solution R1, whereas the I-V curves for TEA$^+$ and choline$^+$, which indicated a smaller conductance, showed a slight "bump" at about 0 mV. Reversal potential was 15 mV. (B) Effects of amiloride (1 mM) or Ni^{2+} (5 mM) upon g_{cat}. As compared with the I-V curve taken in solution RCh, amiloride slightly decreased the current over the whole voltage range, while adding Ni^{2+} to the bath increased currents at positive potentials.

It was also interesting to know whether amiloride or Ni^{2+}, which block the odorant-activated conductance g_{cn} (Fig. 7), had an effect upon I_{cat}. Current voltage relationships of I_{cat} (Fig. 6 B) showed that amiloride reduced I_{cat} only slightly

(13% at −73 mV) and that, with $NiCl_2$ added to the bath, I_{cat} was unaffected or larger, depending on the voltage.

Taken together, the effects of amiloride and Ni^{2+} upon I_{cat} were not comparable with the corresponding effects upon current responses to odorants.

DISCUSSION

In a previous paper (Schild and Bischofberger, 1991) we demonstrated evidence for a calcium-modulated cation conductance g_c in *X. laevis* olfactory neurons. In the meantime, it has been found that some enzymes which influence the concentrations of cAMP and cGMP and thus the cyclic nucleotide-activated conductance g_{cn} are also calcium-dependent (Bredt and Snyder, 1989; Ronnett and Snyder, 1992; Frings, 1993). On the basis of our previously presented data (Schild and Bischhofberger, 1991) it can thus not be ruled out that, at least in part of the experiments, $[Ca^{2+}]_i$ modulated the cyclic nucleotide-activated conductance g_{cn} rather than a second calcium-activated cation conductance g_{cat}. Data which showed that g_{cat} was different from g_{cn} were lacking. A second drawback of our previous study was that $[Ca^{2+}]_i$ was not measured directly and simultaneously with membrane currents. The data given in this paper fill in these gaps.

Herein we have characterized a cation current I_{cat} in olfactory neurons of *X. laevis* which, with various cation compositions of the bath solution (Fig. 6), had reversal potentials of about 15 mV. It was permeable for various cations (Fig. 6) and had no significant Cl^- component (Fig. 4). Its permeability for $[Ca^{2+}]_i$ in solution R1 caused a peripheral increase of $[Ca^{2+}]_i$, which was correlated with the activation of I_{cat} (Figs. 1 and 2). This indicated that g_{cat} was localized in the dendritic knob or in the cilia. Accordingly, I_{cat} was reduced when sucrose was directed through a second pipette onto the cilia while local application of sucrose onto the soma had no effect upon the voltage clamp holding current (Fig. 5).

In *X. laevis*, the current activated by a mixture of citralva and amyl acetate can be blocked by amiloride and Ni^{2+} (Fig. 7). We have also observed that this current can also be reduced by increasing the extracellular calcium concentration (Schild, 1993) and that it is not permeable for choline$^+$ (data not shown). These features do not, however, preclude a chloride contribution to this odorant-gated current (Kurahashi and Yau, 1993). The cyclic nucleotide-activated conductance g_{cn} is also blocked by amiloride and extracellular calcium (Suzuki, 1990, Frings et al., 1992). As amiloride and Ni^{2+} did not have a significant effect upon g_{cat} (Fig. 6 *B*), the conductances underlying the current activated by a mixture of citralva and amyl acetate on the one hand, and I_{cat} on the other, appear to be different. This view is further supported by the facts that 1) choline is permeable for g_{cat} but not for g_{cn} (Kurahashi, 1989) and 2) that I_{cat} had identical amplitudes in 20 μM and 1 mM extracellular calcium (Fig. 4).
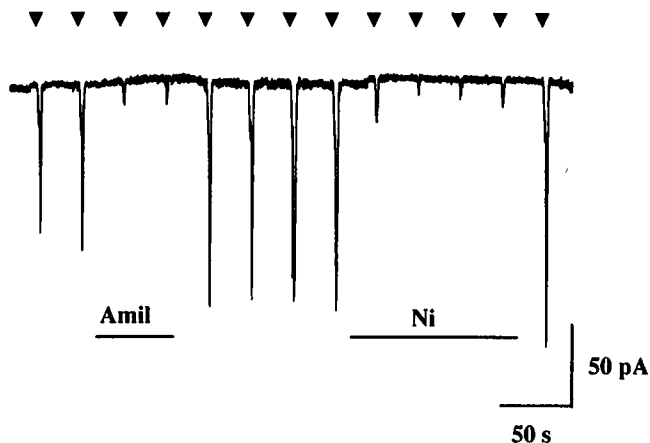

FIGURE 7 Effect of amiloride and Ni^{2+} upon current responses to odor stimuli. Current responses to application of a mixture of citralva (100 μM) and amyl acetate (100 μM) were recorded in the voltage clamp at a holding potential of $u_h = -73$ mV. Pipette solution I2; bath solution R1. Odorants were dissolved in R1 and applied from a second pipette onto the cilia of an olfactory neuron. Where indicated by a bar, amiloride (Amil) or $NiCl_2$ (Ni) were added to the bath solution. In both cases the odorant-induced currents were blocked.

We activated g_{cat} by increasing $[Ca^{2+}]_i$ to values of about 450 nM by replacing extracellular Na^+ by choline$^+$ (Fig. 4). Removal of extracellular Na^+ reverses the sodium gradient across the plasma membrane, thereby forcing sodium gradient-dependent transporters in the reversed mode. The increase of $[Ca^{2+}]_i$ upon removal of Na^+ is therefore most probably due to a Na/Ca-exchanger running in the reversed mode (DiPolo, 1989). This proved to be a suitable experimental tool to activate I_{cat} in a non-transient way. However, g_{cat} could be activated in only 33 of 62 cells. In all other cases, we could increase $[Ca^{2+}]_i$ well above 500 nM, but no change in current (at a voltage clamp potential of −73 mV; $E_K = E_{Cl} = -73$ mV) and no peripheral increase of $[Ca^{2+}]_i$ occurred. g_{cat} seemed thus to be expressed in about half of the cells tested.

The activation of g_{cat} by elevated $[Ca^{2+}]_i$ was presumably not a direct effect since, once activated, g_{cat} appeared to be independent of $[Ca^{2+}]_i$ (Fig. 4) and stayed activated. Therefore g_{cat} is presumably not directly activated by $[Ca^{2+}]_i$. At the moment, the activation mechanism, which could be an activation of a kinase or a phospholipase, as well as the deactivation mechanism, which could be a phosphatase possibly washed out in the whole-cell configuration, remain open questions that are beyond the scope of this paper.

A long-lasting increase in $[Ca^{2+}]_i$ changed the morphological shape of *X. laevis* olfactory neurons (Fig. 2). This change, which did not affect the voltage-gated potassium and sodium currents, can possibly explain one class of isolated olfactory neurons which, after the dissociation procedure, is characterized by a very short dendrite (a few micrometers) or even the absence of a dendrite and the cilia issuing directly from the soma (Schild and Bischofberger, 1991). Whenever g_{cat} was activated in solution R1, the ongoing large current

I_{cat} ($\sim$1 nA) and the increase in $[Ca^{2+}]_i$ up to several micromolar was correlated (100%) with a deterioration in the shape of the cell. The dendrites, some as long as 100 μm, retracted without losing the cilia. This might be due to an osmotic effect or to increased $[Ca^{2+}]_i$ (Mills and Kater, 1990). With choline$^+$ in the bath, currents and increase of $[Ca^{2+}]_i$ were much smaller and changes in the shape of the cell occurred only rarely.

The physiological role of g_{cat} remains to be established. Preliminary evidence suggested that the odorants triethylamine, phenylethylamine, and isovaleric acid increased the IP_3 concentration in a cilia preparation of the main olfactory mucosa of *X. laevis* (Schild et al., 1992) and that a mixture of the same odorants elicited membrane currents in *X. laevis* olfactory neurons (Schild, 1993). Preliminary evidence indicates that g_{cat} is involved in a transduction pathway mediated by both $[Ca^{2+}]_i$ and IP_3 (unpublished observations).

REFERENCES

1. Bacigalupo, J., Morales, B., Ugarte, G., Delgado, R., Jorquera, O., and Labarca, P. 1993. Electrophysiological studies in toad olfactory receptor neurons. *Chem. Senses*. In press.

2. Bredt, D. S., and S. H. Snyder. 1989. Nitric oxide mediates glutamate-linked enhancement of cGMP levels in the cerebellum. *Proc. Natl. Acad. Sci. USA.* 86:9030–9033.

3. Breer, H., T. Klemm, and I. Boekhoff. 1992. Nitric oxide mediated formation of cyclic GMP in the olfactory system. *NeuroReport.* 3:1030–1032.

4. DiPolo, R. 1989. The sodium-calcium exchange in intact cells. *In* Sodium-Calcium Exchange. T. J. A. Allen, D. Noble, and H. Reuter, editors. Oxford University Press, Oxford.

5. Fadool, D. A., and B. W. Ache. 1992. Plasma membrane inositol 1:4,5-triphosphate-activated channels mediate signal transduction in lobster olfactory receptor neurons. *Neuron.* 9:907–918.

6. Firestein, S., B. Darrow, and G. M. Shepherd. 1991. Activation of the sensory current in salamander olfactory receptor neurons depends on a G protein-mediated cAMP second messenger system. *Neuron.* 6:825–835.

7. Firestein, S., and F. S. Werblin. 1989. Odor-induced membrane currents in vertebrate olfactory receptor neurons. *Science (Washington DC).* 244:79–82.

8. Frings, S. 1993. Protein kinase C sensitizes olfactory adenylate cyclase. *J. Gen. Physiol.* 101:183–205.

9. Frings, S., J. W. Lynch, and B. Lindemann. 1992. Properties of cyclic nucleotide-gated channels mediating olfactory transduction. *J. Gen. Physiol.* 100:45–67.

10. Grynkiewicz, G., M. Poenie, and R. Y. Tsien. 1985. A new generation of Ca^{2+} indicators with greatly improved. *J. Biol. Chem.* 260:3440–3450.

11. Hamill, O. P., A. Marty, E. Neher, B. Sakmannn, and F. J. Sigworth. 1981. Improved patch-clamp techniques for high-resolution current recording from cells and cell-free membrane patches. *Pflügers Arch.* 391:85–100.

12. Kleene, S. J., and R. C. Gesteland. 1991. Calcium-activated chloride conductance in frog olfactory cilia. *J. Neurosci.* 11:3624–3629.

13. Kurahashi, T. 1989. Activation by odorants of cation-selective conductance in the olfactory receptor cell isolated from the newt. *J. Physiol. (Lond).* 419:177–192.

14. Kurahashi, T., and K.-W. Yau. 1993. Co-existence of cationic and chloride components in odorant-induced current of vertebrate olfactory receptor cells. *Nature.* 363:71–74.

15. Lischka, F. W., and D. Schild. 1993a. Effects of nitric oxide upon olfactory receptor neurones in *Xenopus laevis. NeuroReport.* 4:582–584.

16. Lischka, F. W., and D. Schild. 1993b. Standing calcium gradients in olfactory receptor neurons can be abolished by amiloride or ruthenium red. *J. Gen. Physiol.* 102:817–831.

17. Lynch, J. W., and B. Lindemann. 1992. Divalent cations decrease sensitivity of cAMP-gated channels to cAMP in rat olfactory receptor cells. ECRO X, München. 1992:96.

18. Marks, P. W., and F. R. Maxfield. 1991. Preparation of solutions with free calcium concentrations in the nanomolar range using 1:2-bis(*o*-aminophenoxy)ethane-*N,N,N',N'*-tetraacetic acid. *Anal. Biochem.* 193:61–71.

19. Mills, L. R., and S. B. Kater. 1990. Neuron-specific and state-specific differences in calcium homeostasis regulate the generation and degeneration of neu cations decrease sensitivity of cAMP-gated channels to cAMP in rat olfactory receptor cells. ECRO X, München. 1992:96.

20. Neher, E., and G. J. Augustine. 1992. Calcium gradients and buffers in bovine chromaffin cells. *J. Physiol.* 450:273–301.

21. Restrepo, D., T. Miyamoto, B. C. Bryant, and J. H. Teeter. 1990. Odor stimuli trigger influx of calcium into olfactory neurons of the channel catfish. *Science (Washington DC).* 249:1166–1168.

22. Restrepo, D., and J. H. Teeter. 1990. Olfactory neurons exhibit heterogeneity in deppolarization-induced calcium changes. *Am. J. Physiol.* 258:C1051-C1061.

23. Restrepo, D., J. H. Teeter, E. Honda, A. G. Boyle, J. F. Marecek, G. D. Prestwich, and D. L. Kalinoski. 1992. Evidence for an InsP$_3$-gated channel protein in isolated rat olfactory cilia. *Am. J. Physiol.* 263:C667–C673.

24. Ronnett, G. V., and S. H. Snyder. 1992. Molecular messengers of olfaction. *Trends Neurosci.* 15:508–513.

25. Schild, D. 1989. Whole-cell currents in olfactory receptor cells of *Xenopus laevis. Exp. Brain Res.* 78:223–232.

26. Schild, D. 1993. Ciliary cation conductances in olfactory receptor cells of the clawed toad *Xenopus laevis. In* Nonselective Cation Channels: Pharmacology, Physiology, and Biophysics. D. Siemen and J. K.-J. Hescheler, editors. Birkhäuser, Basel.

27. Schild, D., and J. Bischofberger. 1991. Ca^{2+} modulates an unspecific cation conductance in olfactory cilia of *Xenopus laevis. Exp. Brain Res.* 84:187–194.

28. Schild, D., I. Boekhoff, F. W. Lischka, and H. Breer. 1992. Signal transduction in olfactory neurons of *Xenopus laevis. In* Rhythmogenesis in Neurons and Networks. Proceedings of the 20th Göttingen Neurobiology Conference. N. Elsner and D. W. Richter, editors. Thieme, Stuttgart.

29. Suzuki, N. 1990. Single cyclic nucleotide activated ion channel activity in olfactory receptor cell soma membrane. *Neurosci. Res. Suppl.* 12:113–126.